Cell, Vol. 122, 221–233, July 29, 2005, Copyright ©2005 by Elsevier Inc. DOI 10.1016/j.cell.2005.05.011

Electron Transfer between Cytochrome c and p66^{Shc} Generates Reactive Oxygen Species that Trigger Mitochondrial Apoptosis

Marco Giorgio,[1,2,8,*] Enrica Migliaccio,[1,2,8] Francesca Orsini,[1,2] Demis Paolucci,[3] Maurizio Moroni,[4] Cristina Contursi,[4] Giovanni Pelliccia,[2] Lucilla Luzi,[2] Saverio Minucci,[1,4] Massimo Marcaccio,[3] Paolo Pinton,[6] Rosario Rizzuto,[6] Paolo Bernardi,[5] Francesco Paolucci,[3] and Pier Giuseppe Pelicci[1,2,7,8,*]

[1] Experimental Oncology Department
European Institute of Oncology
Milan
[2] FIRC Institute of Molecular Oncology
Milan
[3] G Ciamician Chemistry Department
University of Bologna
Bologna
[4] Congenia srl
Milan
[5] Biomedical Sciences Department
University of Padova
Padova
[6] Experimental and Diagnostic Medicine Department
University of Ferrara
Ferrara
[7] Department of Medicine and Surgery
University of Milan
Milan
Italy

Summary

Reactive oxygen species (ROS) are potent inducers of oxidative damage and have been implicated in the regulation of specific cellular functions, including apoptosis. Mitochondrial ROS increase markedly after proapoptotic signals, though the biological significance and the underlying molecular mechanisms remain undetermined. P66^{Shc} is a genetic determinant of life span in mammals, which regulates ROS metabolism and apoptosis. We report here that p66^{Shc} is a redox enzyme that generates mitochondrial ROS (hydrogen peroxide) as signaling molecules for apoptosis. For this function, p66^{Shc} utilizes reducing equivalents of the mitochondrial electron transfer chain through the oxidation of cytochrome c. Redox-defective mutants of p66^{Shc} are unable to induce mitochondrial ROS generation and swelling in vitro or to mediate mitochondrial apoptosis in vivo. These data demonstrate the existence of alternative redox reactions of the mitochondrial electron transfer chain, which evolved to generate proapoptotic ROS in response to specific stress signals.

Introduction

Apoptosis is essential for the maintenance of tissue homeostasis, and its deregulation is implicated in cancer, degenerative diseases, and aging. Mitochondria play a central role in apoptosis. They contain a number of proapoptotic factors, such as cytochrome c (cyt c), aif, smac/diablo, and endoG, which are released into the cytosol during apoptosis, where they activate a series of enzymatic activities that lead to the specific degradation of proteins and DNA (Danial and Korsmeyer, 2004; Pelicci, 2004).

The release of proapoptotic factors from mitochondria is due to the disruption of the organelle integrity, which is achieved through multiple and concomitant events. In the case of cyt c, for example, its release requires permeabilization of the outer membrane, remodeling of the mitochondrial *cristae*, and dissociation of cyt c from cardiolipin, a constituent of the inner membrane (Green and Kroemer, 2004). These events are triggered by the opening of a high-conductance channel, the permeability transition pore (PTP) (Bernardi et al., 2001). Opening of the PTP provokes an increase of inner membrane permeability to ions and solutes (the so-called permeability transition, PT), followed by net water influx toward the mitochondrial matrix, swelling of the organelle, and physical rupture of its outer membrane, with the consequent release of proteins of the intermembrane space, including cyt c (Bernardi et al., 2001). Another mechanism leading to alterations of the mitochondrial membrane integrity is the translocation of proapoptotic proteins such as Bax and Bid from the cytosol to the outer mitochondrial membrane, where they form channels and/or regulate the function of preexisting channels (Scorrano and Korsmeyer, 2003). Whether these events then trigger the PT or are per se sufficient to mediate complete cyt c release remains, however, controversial.

Reactive oxygen species (ROS; superoxide, hydrogen peroxide, and hydroxyl radicals) are potent intracellular oxidants, which have been proposed as critical regulators of apoptosis (Danial and Korsmeyer, 2004). Indeed, ROS induce the opening of the PTP through oxidation-dependent mechanisms and are potent inducers of apoptosis, both in cultured cells and in vivo (Petronilli et al., 1994; Danial and Korsmeyer, 2004). Beyond their documented proapoptotic activity when administered exogenously, endogenously produced ROS are implicated in the execution of the apoptotic program itself, regardless of the type of triggering signal. In fact, a marked increase of intracellular ROS is consistently associated with apoptosis, and treatments with antioxidants protect cells from apoptosis (Mayer and Noble, 1994).

The molecular mechanisms underlying increased ROS generation during apoptosis are unclear. It has been proposed that ROS accumulation is secondary to the progress of the apoptotic process and is caused by the interruption of the mitochondrial electron transfer chain (ETC), a consequence of the PT and of cyt c release (Cai and Jones, 1998). Alternatively, ROS might function to trigger mitochondrial apoptosis, serving as signaling molecules to initiate the PT. Notably, intracellular ROS arise prior to cyt c release during the acti-

*Correspondence: marco.giorgio@ifom-ieo-campus.it; piergiuseppe.pelicci@ifom-ieo-campus.it
[8] These authors contributed equally to this work.

vation of several apoptotic pathways, such as those involving p53 or TNFα or those triggered by hyperglycemia, ischemia/reperfusion, or viral infection (Trinei et al., 2002; Sakon et al., 2003; Brownlee, 2001; Becker, 2004).

ROS are generated accidentally, as by products of aerobic metabolism, and mitochondria are the major source of intracellular ROS (Wallace, 1999). During respiration, electrons are extracted from substrates and are then transferred to molecular oxygen through a chain of enzymatic complexes (I–IV). In the final step of the ETC, cyt c oxidase (COX; complex IV) ensures the reduction of molecular oxygen to water, without formation of oxygen radicals. However, partial reduction of oxygen with generation of ROS can occur if molecular oxygen interacts with the ETC upstream of complex IV. Experimental data indicate that ROS are indeed continuously produced during mitochondrial respiration and that up to 2% of the total oxygen consumption is converted to ROS (Chance et al., 1979). How ROS are regulated during apoptosis is unclear.

$P66^{Shc}$ deletion in mice ($p66^{Shc-/-}$) decreases the incidence of aging-associated diseases, such as atherosclerosis, and prolongs life span (Migliaccio et al., 1999; Napoli et al., 2003; Francia et al., 2004). The underlying molecular mechanisms are, however, unknown. $P66^{Shc}$ is a splice variant of $p52^{Shc}$/$p46^{Shc}$, two cytoplasmic adaptor proteins involved in the propagation of intracellular signals from activated tyrosine kinases to Ras (Pelicci et al., 1992). $P66^{Shc}$ has the same modular structure of $p52^{Shc}$/$p46^{Shc}$ (SH2-CH1-PTB) and contains a unique N-terminal region (CH2); however, it is not involved in Ras regulation but rather functions in the intracellular pathway(s) that regulates ROS metabolism and apoptosis (Migliaccio et al., 1997; Migliaccio et al., 1999; Trinei et al., 2002).

Intracellular ROS levels are decreased in $p66^{Shc-/-}$ cells, as revealed by the reduced oxidation of ROS-sensitive probes and the reduced accumulation of endogenous markers of oxidative stress (8-oxo-guanosine) (Trinei et al., 2002; Francia et al., 2004). Likewise, $p66^{Shc-/-}$ mice have diminished levels of both systemic (isoprostane) and intracellular (nytrotyrosines, 8-oxo-guanosine) oxidative stress (Napoli et al., 2003; Francia et al., 2004; Trinei et al., 2002).

$P66^{Shc-/-}$ cells are resistant to apoptosis induced by a variety of different signals, including hydrogen peroxide, ultraviolet radiation, staurosporine, growth factor deprivation, calcium ionophore, and CD3-CD4 cross-linking (Migliaccio et al., 1999; Orsini et al., 2004; Pacini et al., 2004). Similarly, the $p66^{Shc-/-}$ mice are resistant to apoptosis induced by paraquat, hypercholesterolemia, and ischemia (Migliaccio et al., 1999; Napoli et al., 2003; Zaccagnini et al., 2004).

Expression of $p66^{Shc}$ is indispensable for the mitochondrial depolarization and the release of cyt c observed after treatment of cells with various proapoptotic signals, suggesting that it regulates the mitochondrial pathway of apoptosis. Since inhibition of PTP opening blocks the proapoptotic function of $p66^{Shc}$, the PTP itself might be the target of $p66^{Shc}$ activity (Trinei et al., 2002; Orsini et al., 2004). We report here that $p66^{Shc}$ is a redox enzyme that generates mitochondrial hydrogen peroxide for the induction of PT and apoptosis.

Results

$P66^{Shc}$ Induces Permeability Transition of Isolated Mitochondria

To investigate whether the effect of $p66^{Shc}$ on the mitochondrial PTP is direct, we analyzed its ability to induce swelling of purified mitochondria, measured as decrease of light absorbance of the organelle suspension. Mitochondria were purified from wild-type (wt) mouse liver and pretreated with a low concentration of Ca^{2+} (7 μM), a condition that does not induce PT but sensitizes PTP opening to other signals (Bernardi et al., 2001). Addition of recombinant $p66^{Shc}$ (5–20 μM) did not induce swelling, as compared to a large load of Ca^{2+} (0.2 mM), a well-characterized inducer of the PT (Figure 1A). Since $p66^{Shc}$ is not imported by mitochondria in vitro (Ventura et al. 2004), this finding indicates that $p66^{Shc}$ is unable to alter mitochondrial permeability when acting from the outside of the organelle.

We then investigated the effect of $p66^{Shc}$ on the PTP when the protein is allowed to enter the mitochondrial intermembrane space. To this end, we treated purified mitochondria with a low concentration of digitonin (25 μM), which selectively permeabilizes the outer membrane without affecting PT, as shown by the fact that digitonin-treated mitochondria retain cyt c, respire, and are sensitive to Ca^{2+}-induced swelling (Diwan et al. [1988] and data not shown). Under these conditions, addition of recombinant $p66^{Shc}$ induced marked and dose-dependent swelling of mitochondria (Figure 1B). This effect was abolished in the absence of respiratory substrates, indicating that it depends on an intact transmembrane potential (data not shown). Furthermore, it was Ca^{2+} dependent (data not shown) and comparable to that obtained by exogenously added ROS (H_2O_2; Figure 1C). Notably, $p66^{Shc}$ was unable to induce swelling when digitonin-treated mitochondria were pretreated with PT inhibitors such as cyclosporine A (CsA), a drug that binds the PTP component cyclophilin D, or N-ethyl-maleimide (NEM), a sulfhydryl reagent that blocks PTP opening by thiol oxidants (Petronilli et al., 1994) (Figure 1D). These results suggest that $p66^{Shc}$ is biologically active when it localizes within the mitochondrial intermembrane space, where it induces PT through oxidation-dependent mechanisms.

$P66^{Shc}$ Localizes within the Mitochondrial Intermembrane Space

$P66^{Shc}$ is enriched in the submitochondrial fraction containing inner membranes (Orsini et al., 2004). To further investigate its localization, mitochondria preparations from MEFs (Figure 1E) were treated with digitonin (which allows extraction of soluble proteins from the intermembrane space) or digitonin and high salt (which extracts membrane bound proteins). After centrifugation, the resulting pellets and supernatants were analyzed by Western blotting (WB) by using anti-$p66^{Shc}$, anti-cyt c, anti-mtHsp70, or anti-porin antibodies. Digitonin or digitonin/high-salt treatments did not modify

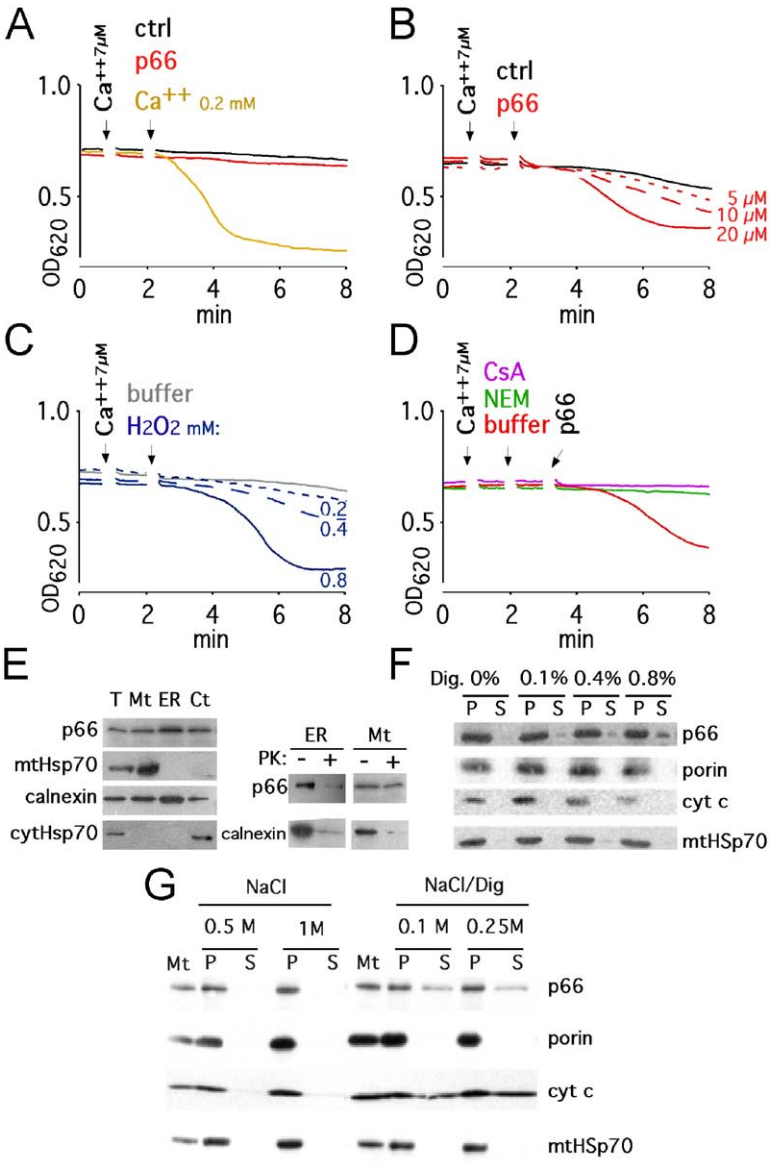

Figure 1. P66Shc Localizes within the Mitochondrial Intermembrane Space and Induces Swelling of Isolated Mitochondria

Absorbance changes of purified liver mitochondria, either intact (A) or treated with 25 μM digitonin (B–D), pretreated with 7 μM $CaCl_2$ and supplemented with the following: (A) 20 μM collagenase as inactive control (control [ctrl]; black trace), 20 μM p66Shc (red), or 200 μM $CaCl_2$ (brown); (B) 20 μM collagenase in 0.25 M sucrose (ctrl, black) or different concentrations of p66Shc (5, 10, and 20 μM, as indicated; red); (C) different concentrations of H_2O_2 (blue) or control buffer (gray); (D) 20 μM p66Shc (added to all kinetics) and 1 μM CsA (violet), 20 μM NEM (green) or control buffer (red). Each experiment was performed six times using different mitochondrial preparations and two distinct preparations of the p66Shc. (E) (Left panels) WB analysis of MEF subcellular fractions using anti-p66Shc, anti-mtHp70, anti-calnexin, and anti-cytoplasmic Hsp70 antibodies. T, total extract; Mt, mitochondria; ER, endoplasmic reticulum; Ct, cytosol. (Right panels) ER and Mt fractions were treated with Proteinase K (PK) and analyzed by WB with anti-calnexin or anti-p66Shc antibodies. (F and G) Mitochondrial fractions from MEFs were treated with the indicated concentrations of NaCl and/or digitonin. After centrifugation, pellets (P) and supernatants (S) were analyzed by WB.

the localization of porin (a marker of the outer membrane) and of mtHsp70 (matrix), indicating that these experimental conditions did not provoke gross structural alterations of purified mitochondria (Figures 1F and 1G). As expected, digitonin/high salt but not digitonin alone induced cyt c release in the supernatant (Griparic et al., 2004). P66Shc, instead, was partially and equally released by either digitonin or digitonin/high salt, suggesting that it exists within the inner mitochondrial space in the form of both soluble and nonsoluble protein (mitochondrial p66Shc is about 50 ng/mg of total proteins; see Figure S1 in the Supplemental Data available with this article online). Similar results were obtained by morphometric analysis of immunoelectron microscopy sections of wt MEFs, which revealed association of mitochondrial gold particles with the inner membrane (55.7%), intermembrane space (35.4%), and matrix (8.9%) (data not shown).

P66Shc Stimulates Generation of ROS by Energized Mitochondria

P66Shc expression is indispensable for the upregulation of intracellular ROS during p53- or ischemia-induced apoptosis (Trinei et al., 2002; Pacini et al., 2004; Zaccagnini et al., 2004). To investigate whether p66Shc-regulated ROS derive from mitochondria, we analyzed intact liver mitochondria from wt or $p66^{Shc-/-}$ mice upon treatment with carbon tetrachloride (CCl_4; 2 mg/kg), a chemical that induces ROS- and p66Shc-dependent apoptosis. We had previously shown that in vivo treatment with CCl_4 induces apoptosis of hepatocytes in wt but not $p66^{Shc-/-}$ mice and that apoptosis in wt animals is prevented by treatment with the antioxidant N-acetyl cysteine. Likewise, CCl_4 induces p66Shc- and ROS-dependent apoptosis of MEFs (Figure S2). Liver mitochondria were collected 20 hr after treatment, and ROS were measured by spectrofluorimetry, using a mole-

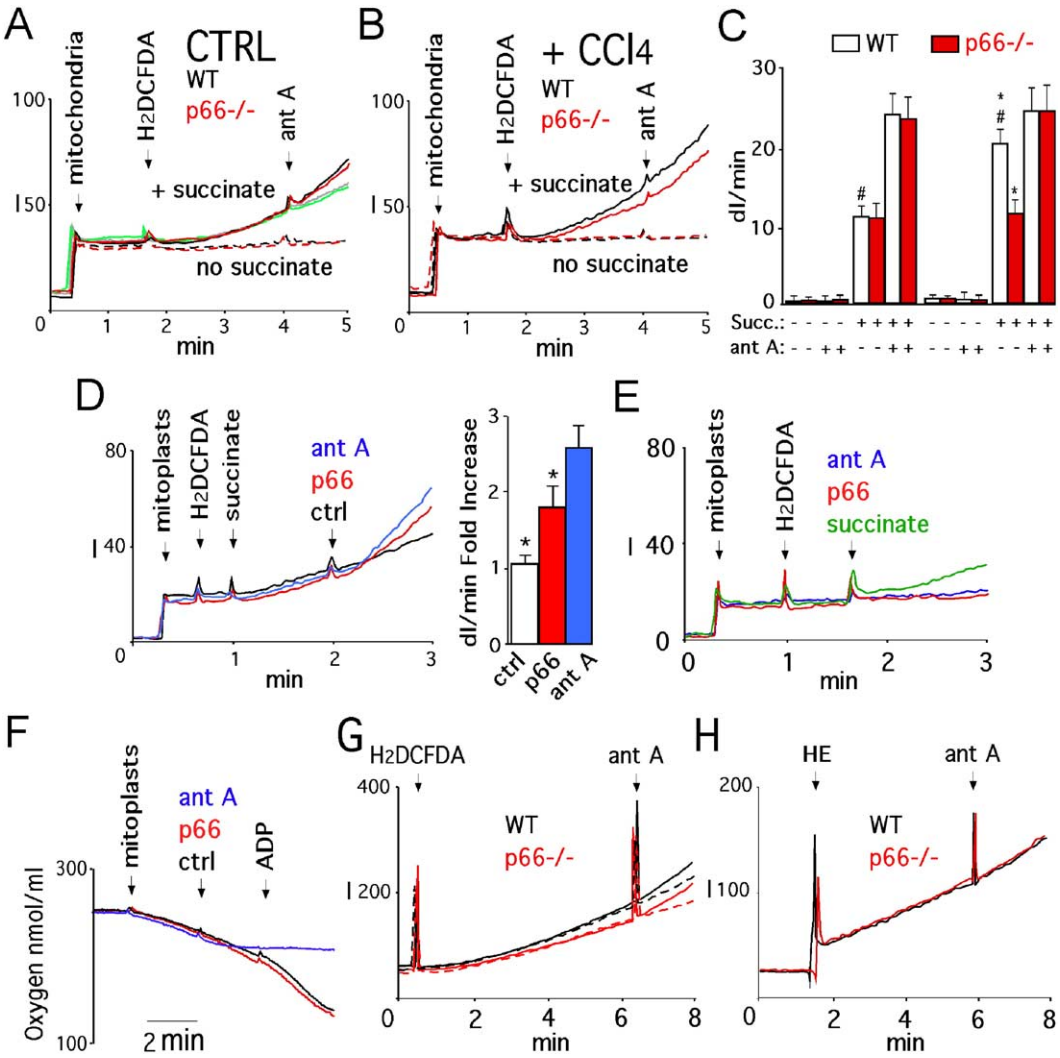

Figure 2. P66^{Shc} Stimulates Mitochondrial Generation of ROS

(A and B) Fluorescence changes (ex. 498, em. 527; I, intensity of fluorescence) and corresponding bar graph (rate of fluorescence intensity/min) (C) of mitochondria from wt (black lines in [A] and [B] and empty bars in [C]) or p66$^{Shc-/-}$ (red lines and red bars) mouse livers, treated with placebo ([A], CTRL) or CCl_4 ([B], +CCl_4), after sequential additions of H_2DCFDA and ant A (black and red lines) or control ethanol (gray line, wt; green line, p66$^{Shc-/-}$) with (plain) or without (dashed) succinate. (A) and (B) report one set of experiments representative of four; (C) reports the average of the four experiments ± SEM (#, wt ctrl versus wt +CCl_4, $p < 0,01$; #, p66$^{Shc-/-}$ + CCl_4 versus wt + CCl_4, $p < 0.01$). Respiration was controlled for each mitochondrial preparation. (D) Fluorescence changes (ex. 498, em. 527) of purified liver mitoplasts after sequential additions of H_2DCFDA, succinate and ant A (blue), p66^{Shc} (red), or 20 μM collagenase (ctrl, black). (D) reports one set of experiments. The average of six experiments is reported in the graph of the right panel ± SEM, where results are expressed as fold increase in fluorescence rate induced by p66^{Shc}, ant A, or control buffer (*, p66^{Shc} versus ctrl, $p < 0.01$). (E) Fluorescence changes (ex. 498, em. 527) of purified liver mitoplasts after sequential additions of H_2DCFDA and succinate (green), p66^{Shc} (red), or ant A (blue). (F) Respiration analysis of mitoplasts after additions of p66^{Shc} (red), ant A (blue), or control buffer (ctrl, black). ADP (100 μm) was added to all samples to maximize respiration. (G and H) Fluorescence changes in intact wt (black) or p66Shc$^{-/-}$ (red) MEFs incubated with H_2DCFDA (G) or HE (ex. 410, em. 490) (H) and treated with ant A (plain) or ethanol as control (dashed).

cular probe that becomes fluorescent upon oxidation by ROS (2′,7′-dichlorofluorescin diacetate; H_2DCFDA) (LeBel et al., 1992). The rate of mitochondrial H_2DFCDA oxidation increased significantly after CCl_4 treatment in the wt mice, while it remained unchanged in the p66$^{Shc-/-}$ mice (Figures 2A–2C). Notably, H_2DCFDA oxidation was consistently detected only in the presence of respiratory substrates, such as succinate (Figures 2A–2C) or glutamate/malate (data not shown). Together, these findings indicate that p66^{Shc} expression is indispensable for the increased generation of mitochondrial ROS after challenge with proapoptotic stimuli and that p66^{Shc} requires a functional ETC for this activity.

To analyze the mechanisms underlying the regulatory effect of p66^{Shc} on mitochondrial ROS generation, we first investigated ROS scavenging. The total peroxide scavenging activities in mitochondrial preparations from wt and p66$^{Shc-/-}$ mouse livers were comparable (Figure S3). Furthermore, we found no differences in any of the known ROS scavenging systems (catalase, SODs, and

GSH-peroxidase) in samples from wt or p66$^{Shc-/-}$ fibroblasts and tissues (Figure S3), suggesting that the effect of p66^{Shc} on mitochondrial ROS is due to increased ROS production rather than diminished scavenging.

The effect of p66^{Shc} on mitochondrial ROS production might be direct or, rather, be the consequence of the organelle swelling induced by p66^{Shc}. To distinguish between these two possibilities, we investigated the effect of recombinant p66^{Shc} on ROS generation by purified mitoplasts. Mitoplasts are unable to swell after PTP opening, yet they respire (due to a fraction of cyt c that remains associated to the inner membrane; Figure 2F). Strikingly, addition of recombinant p66^{Shc} to mitoplasts increased H_2DCFDA oxidation (Figure 2D). These data indicate that the effect of p66^{Shc} on mitochondrial ROS production is not a consequence of the organelle swelling and suggest that p66^{Shc} directly stimulates mitochondrial ROS generation.

P66^{Shc} Produces Mitochondrial Hydrogen Peroxide without Inhibiting Respiration

Mitochondrial respiration generates hydrogen peroxide (H_2O_2) by dismutation of superoxide anion ($O_2^{\cdot-}$), which is produced by reduction of oxygen by semiquinone (Balaban et al., 2005). A well-characterized mechanism leading to mitochondrial ROS generation is inhibition of ETC downstream to quinone. Antimycin A (ant A), for example, blocks the ETC at the level of complex III and is a potent inducer of $O_2^{\cdot-}$ and H_2O_2 production (Balaban et al., 2005). Therefore, we investigated the effects of p66^{Shc} on mitochondrial respiration and $H_2O_2/O_2^{\cdot-}$ metabolism.

Like ant A, p66^{Shc} did not induce ROS production in nonrespiring mitochondria (data not shown) or mitoplasts (Figures 2D and 2E). Unlike ant A, however, p66^{Shc} did not decrease oxygen consumption of mitoplasts (Figure 2F) or mitochondria (data not shown), indicating that it does not block respiration. To obtain in vivo confirmation, oxygen consumption was measured in purified liver and heart mitochondria and in intact primary fibroblasts from wt and p66$^{Shc-/-}$ mice under either basal or uncoupled conditions and using different substrates. In no case did we observe significant differences in respiration between wt and p66$^{Shc-/-}$ mitochondria (data not shown).

To characterize ROS production by p66^{Shc}, we used H_2DCFDA or hydroetidine (HE), two fluorescent probes that are oxidized by H_2O_2 or $O_2^{\cdot-}$, respectively (LeBel et al., 1992; Zhao et al., 2003). Their specificity in our experimental system was confirmed by the findings that basal and p66^{Shc}-induced H_2DCFDA oxidation by mitoplasts was inhibited by catalase (an H_2O_2 scavenger) but not by superoxide dismutase (SOD) (which generates H_2O_2 from $O_2^{\cdot-}$), while HE oxidation was inhibited by SOD but not by catalase (Figure S4). Analysis of basal and ant A-induced oxidation of H_2DCFDA or HE in wt and p66$^{Shc-/-}$ MEFs (Figures 2G and 2H) and purified liver mitochondria (data not shown) revealed decreased levels of H_2O_2 but not $O_2^{\cdot-}$ in the p66$^{Shc-/-}$ samples. It appears, therefore, that p66^{Shc} stimulates H_2O_2 generation without affecting mitochondrial respiration or production of $O_2^{\cdot-}$. Since, however, it requires a functional ETC, these data suggest that p66^{Shc} favors oxygen reduction using reducing equivalents from the respiratory chain. We estimate the rate of H_2O_2 production by p66^{Shc} in the range of 10 nM/min/mg of mitochondrial protein, both in vivo (Figures 2A and 2B) and in vitro (Figure 2D) (using standard curves of H_2O_2-induced H_2DFCDA fluorescence in mitoplasts or mitochondria suspensions; data not shown).

P66^{Shc} Is a Redox Protein that Mediates Electron Transfer

We therefore investigated whether p66^{Shc} is capable itself to execute an electron transfer (ET) reaction. To this end, we measured the ability of recombinant p66^{Shc} to mediate ET when adsorbed onto a probe electrode by cyclic voltammetry (CV) (Armstrong, 2002). Protein adsorption was performed through the carboxylic group of 11-mercaptoundecanoic acid self-assembled as a monolayer (SAM) onto a gold electrode. In the absence of adsorbed proteins, the CV curve reflected the unperturbed and symmetrical capacitive response of the SAM electrode to alternate oxidation and reduction scans, which is typical of long-chain alkylthiols SAMs (Figure 3A, left panel). Accordingly, baseline subtraction from the oxidation and reduction scans resulted to zero (Figure 3A upper panel; red line). Strikingly, when the SAM electrode was coated with recombinant p66^{Shc}, the two CV scans were modified by the superimposition of additional oxidation and reduction events, in the regions of 100 and –170 mV, respectively. Baseline subtraction resulted in two sharp peaks (Figure 3A). The intensity of the two peaks was always proportional to the scan rate (data not shown). Furthermore, the calculated concentration of p66^{Shc} that contributed to the faradaic ET reaction was about 6 pmol/cm^2, consistent with a homogenous and thin layer of an electrode-coated protein of about 66 kDa. These data indicate that electrode-coated p66^{Shc} undergoes an ET process.

P66^{Shc} Oxidizes Cyt c In Vitro

The average of the oxidation and reduction peaks is a direct measure of the redox potential of an ET protein, which, in the case of p66^{Shc}, is about –35 mV. Among the redox systems that are present within the mitochondria, the redox value of cyt c (17 mV) is one of the closest to that of p66^{Shc} (Figure 3A and Chen et al. [2002]). Therefore, we evaluated whether cyt c and p66^{Shc} can exchange electrons. Absorption of cyt c (but not of glucose oxidase, used as negative control; data not shown) on the p66^{Shc}-coated electrode provoked a dramatic change of its CV response (Figure 3B). First, the reduction/oxidation peaks typical of p66^{Shc} were no longer detected, while a novel, single ET event was recorded with a redox potential of 10 mV (Figure 3B), distinct from that of either p66^{Shc} or cyt c alone (Figure 3A). Second, the calculated electrode capacitance of p66^{Shc} was reduced of about 30% in the presence of cyt c, suggesting that cyt c formed an additional film onto the p66^{Shc}-coated SAM electrode. These findings indicate that p66^{Shc} and cyt c interacted physically and were integrated in the same ET event. Finally, the reduction and oxidation peaks of p66^{Shc} became much closer in the presence of cyt c (from 270 to 35 mV),

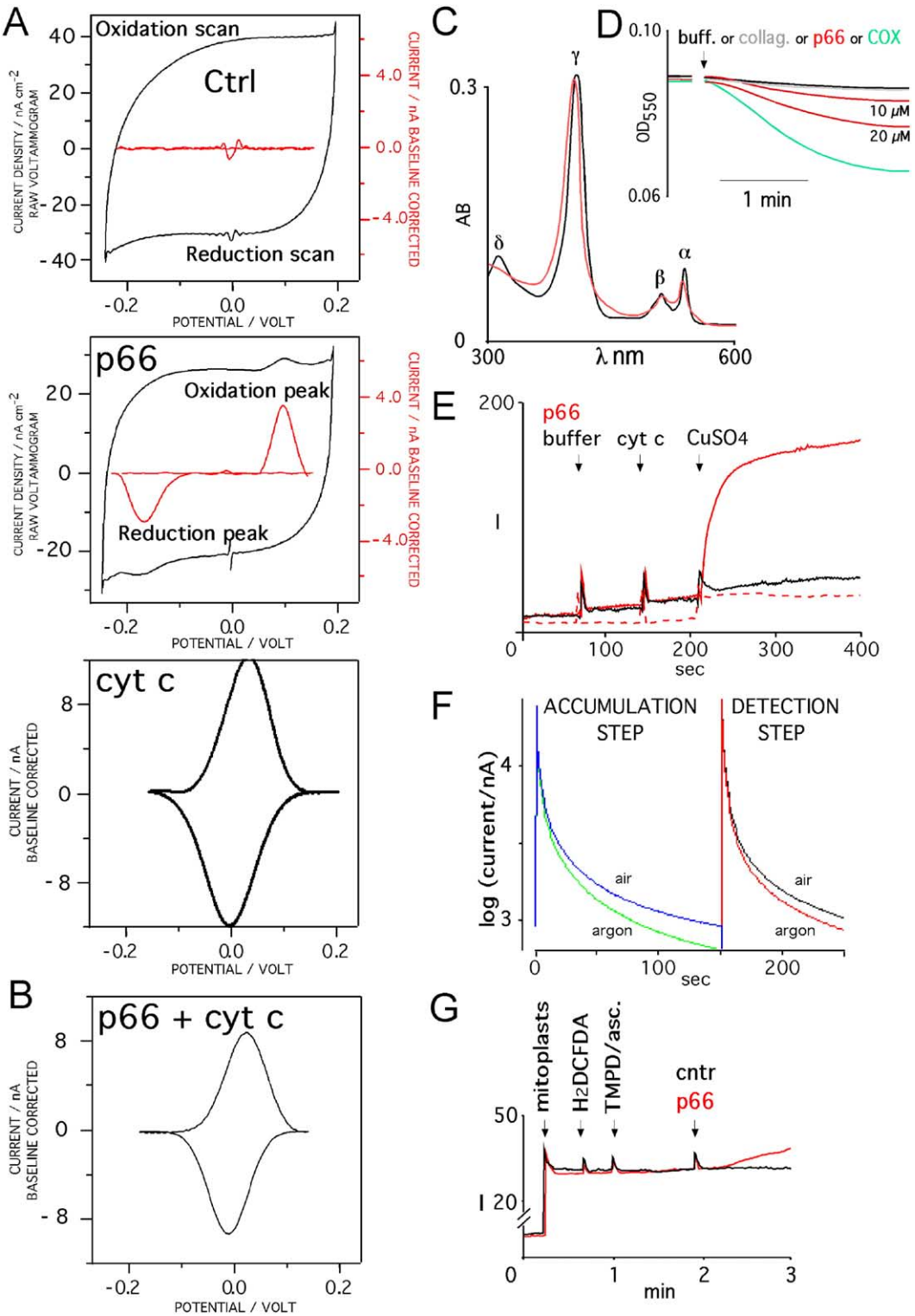

Figure 3. Redox Properties of p66^{Shc} and of the p66^{Shc}-Cyt c Couple

(A) CV experiments using uncoated (upper panel, Ctrl), p66^{Shc} (middle panel)-, or cyt c (lower panel)-coated SAM electrodes.

(B) CV experiment using a p66^{Shc}-coated SAM electrode in the presence of cyt c.

(C) Absorption spectrum of reduced cyt c in the presence of 20 μM p66^{Shc} (red) or control buffer (black).

(D) Absorbance changes at 550 nm of reduced cyt c in the presence of the indicated concentrations of recombinant p66^{Shc} (red), yeast-purified COX (green), control buffer (black), or 20 μM collagenase (gray line).

(E) Fluorescence changes of a 20 μM H_2DCFDA solution during the sequential addition of 20 μM p66^{Shc} (red) or control buffer (black), 10 μM reduced cyt c, and 50 μM $CuSO_4$.

indicating that the ET kinetics of p66Shc is accelerated by cyt c. Therefore, it appears that p66Shc executes a redox reaction with cyt c under the CV experimental conditions.

We then investigated the effect of p66Shc on the redox status of cyt c by spectrophotometry. Addition of p66Shc modified the absorbance spectrum of reduced cyt c, provoking a slight shift of the γ peak and a reduction of the amplitude of the α peak (Figure 3C). These modifications are consistent with a strong interaction between p66Shc and the prosthetic group of cyt c, and the partial oxidation of cyt c. Analysis of the kinetics of absorbance at 550 nm (α peak) revealed that the effect of p66Shc on cyt c oxidation status is dose dependent and comparable to that of purified yeast COX (Figure 3D). Together, these findings indicate that p66Shc is a redox protein that oxidizes cyt c in vitro.

Electron Transfer between p66Shc and Cyt c Generates Hydrogen Peroxide In Vitro

We then investigated whether p66Shc oxidizes H_2DCFDA when reacting with cyt c. Addition of p66Shc to reduced cyt c did not provoke H_2DFCDA oxidation (data not shown). A significant fluorescence boost from oxidized H_2DCFDA was, instead, recorded in the presence of copper (but not zinc or iron) ions (Figure 3E; red trace), indicating that, in vitro, the copper atom catalyzes generation of free radicals from the redox center of the p66Shc-cyt c complex. Notably, under anoxic conditions, H_2DCFDA oxidation was significantly decreased, suggesting a role for oxygen intermediates in this process (Figure 3E; dashed trace). Since H_2DCFDA oxidation is specifically sensitive to H_2O_2, these data suggest that this is the molecular species that forms during the reaction.

To obtain a direct proof that H_2O_2 is generated during the electrochemical reaction of p66Shc with cyt c, we measured current generation at 650 mV (which corresponds to the oxidation potential of H_2O_2) in an electrode-confined p66Shc-cyt c system (Callegari et al., 2004). P66Shc and cyt c were entrapped within a conducting polymeric film and immobilized onto a glassy carbon electrode. The coated electrode was then transferred into an air- or argon-saturated phosphate buffer and a –100 mV potential applied for 150 s (this potential induces the continuous reduction of the p66Shc-cyt c complex, has no direct effect on molecular oxygen, and allows accumulation of oxygen radicals, if formed, in the gel; accumulation step, Figure 3F). Analysis of current generation at –100 mV revealed early oxygen reduction current generated by the p66Shc/cyt c electrode, only in the presence of air-saturated buffer (Figure 3F; left panel). After switching of the electrode potential to 650 mV (to measure accumulated H_2O_2; detection step, Figure 3F), current was recorded specifically in the presence of air-saturated buffer (Figure 3F; right panel). Furthermore, when the initial potential was set at +100 mV (which cannot reduce the p66Shc/cyt c redox center), neither catalytic oxygen reduction nor H_2O_2 oxidation was detected (data not shown). Together, these results provide direct demonstration that ET between p66shc and cyt c leads to oxygen reduction and formation of H_2O_2.

P66Shc Generates Hydrogen Peroxide from Reduced Cyt c In Vivo

We then investigated whether, in vivo, the ETC site of p66Shc-induced ROS production is compatible with the described in vitro activity of p66Shc on reduced cyt c. To this end, mitochondria were treated with ascorbate/N,N′-tetramethyl-p-phenyldiamine (TMPD) in the absence of energetic substrates. Under these experimental conditions, mitochondrial respiration is supported by reduction of cyt c (by TMPD), while complexes I–III remain inactive. As expected, since the ETC sites of ROS production are excluded in this system, ascorbate/TMPD-treated mitochondria did not generate detectable ROS (Figure 3G; black trace). Addition of recombinant p66Shc, instead, induced H_2DFCDA oxidation, indicating that p66Shc is able to generate ROS by acting downstream to reduced cyt c. Consistently, p66Shc did not increase ROS generation induced by inhibitors of complexes I (rotenone) or III (ant A) (Figure S4).

Mapping of the Redox Center of p66Shc

To map the region of p66Shc interacting with cyt c, we compared, by ELISA, the cyt c binding properties of p66Shc with those of p52Shc or p46Shc, which are not involved in the regulation of ROS and apoptosis (Migliaccio et al., 1999). Increasing amounts of coated cyt c (0.25–4 μg) were incubated with increasing amounts of Shc proteins (0.08–4 μg) and bound proteins revealed with anti-Shc antibodies. The p66Shc-cyt c association was dose dependent at each concentration of the two proteins (Figure 4B). A residual binding activity (about 10%) was detected for p52Shc, while p46Shc did not bind at all, suggesting that the N-terminal region of p66Shc (CH2-PTB) is involved in cyt c binding.

To narrow down the cyt c binding region of p66Shc, we expressed various portions of the CH2-PTB region as GST fusion proteins (Figure 4C) and measured their ability to recover cyt c from cellular lysates through pull-down experiments. Results showed that a 52 amino acid region N terminal to the PTB domain is critical for the binding to cellular cyt c (denominated CB, for cyt c binding; Figures 4A and 4C). This region is highly conserved among the known p66Shc vertebrate orthologs (Figure 4D) and contains glutamic (E125, E132, E133) and tryptophan (W134 and W148) residues, which, in the context of COX IV and yeast cyt c peroxidase, are essential for the interaction and ET reaction

(F) Current measurement at –100 (accumulation step) or +650 (detection step) mV of the glassy carbon electrode coated with a gel containing p66Shc and cyt c. Recordings were performed in aerated (air, blue and black traces) or argon-flushed (argon, green and red traces) phosphate buffer, as indicated.

(G) Fluorescence changes of purified liver mitoplasts after sequential additions of H_2DCFDA, 0.5 mM ascorbate, 0.2 mM TMPD, and p66Shc (red) or control buffer (black).

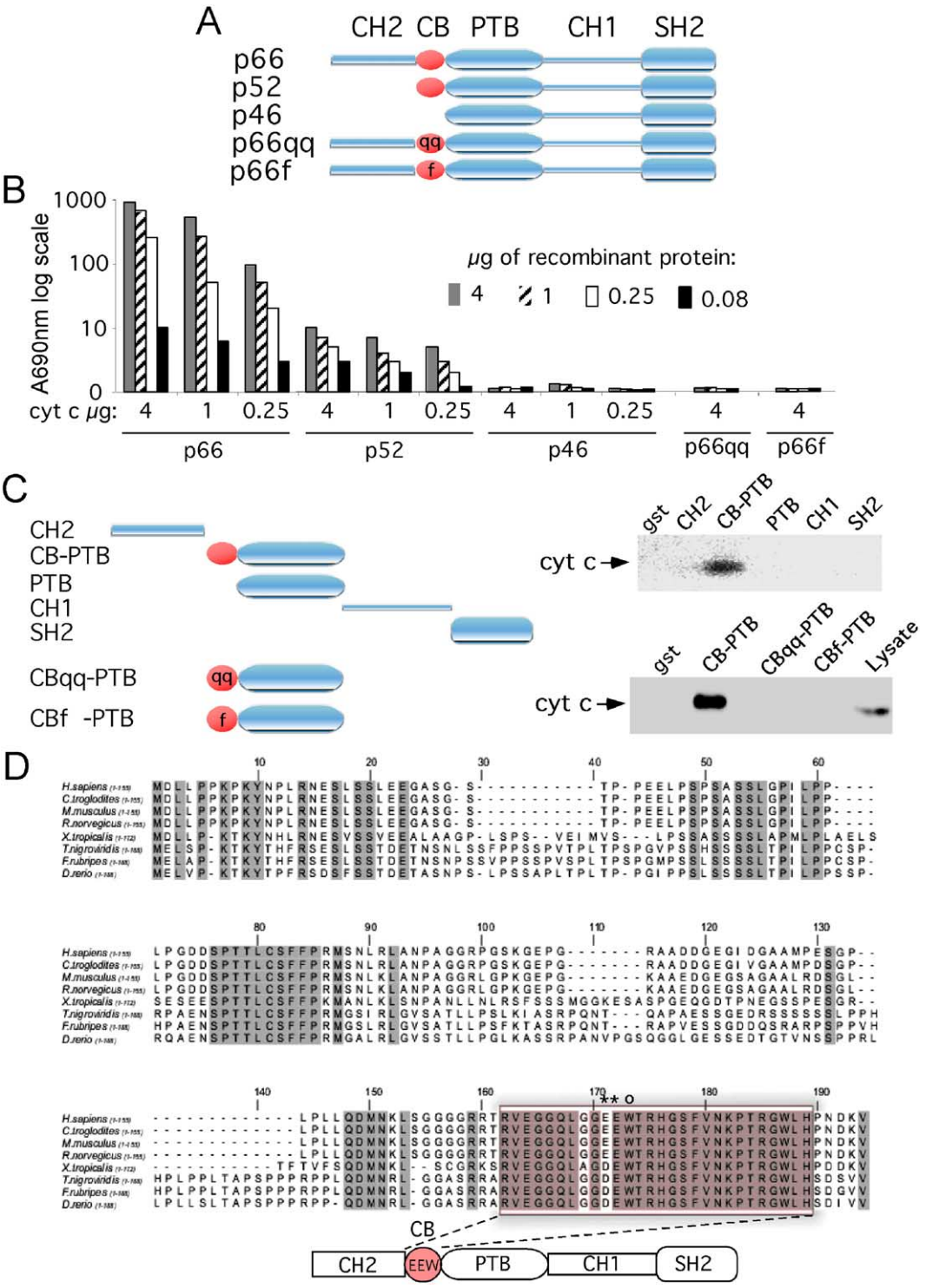

Figure 4. Mapping of the p66^{Shc} Cyt c-Interacting Region

(A) Modular organization of Shc proteins (p66, p52, p46) and p66^{Shc} mutants (*qq* and *f*). The positions of the *qq* and *f* mutations are indicated within the CB region.

(B) ELISA binding assay of recombinant p66^{Shc}, p52^{Shc}, p46^{Shc}, p66^{Shc}*qq*, and p66^{Shc}*f* proteins added at different concentrations to dish wells preadsorbed with different concentrations of cyt c, as indicated.

(C) In vitro pull-down experiment (right panel) using MEF lysates and the schematized (left panel) portions of p66^{Shc} expressed in bacteria as GST fusion proteins. Recovered proteins were analyzed by Western blotting using anti-cyt c antibodies.

(D) Amino acid sequence of the p66^{Shc} N-terminal region. Amino acid sequence alignment of the CH2-PTB N-terminal regions (aa 1–155) of the available p66^{Shc} vertebrate horthologs. Identities are highlighted in gray. The most conserved region (CB) is boxed in red. The relevant glutamic (E132 and E133) and triptophan (W134) residues are indicated in the sequence (by asterisks and circle, respectively) and in the p66^{Shc} modular organization scheme below.

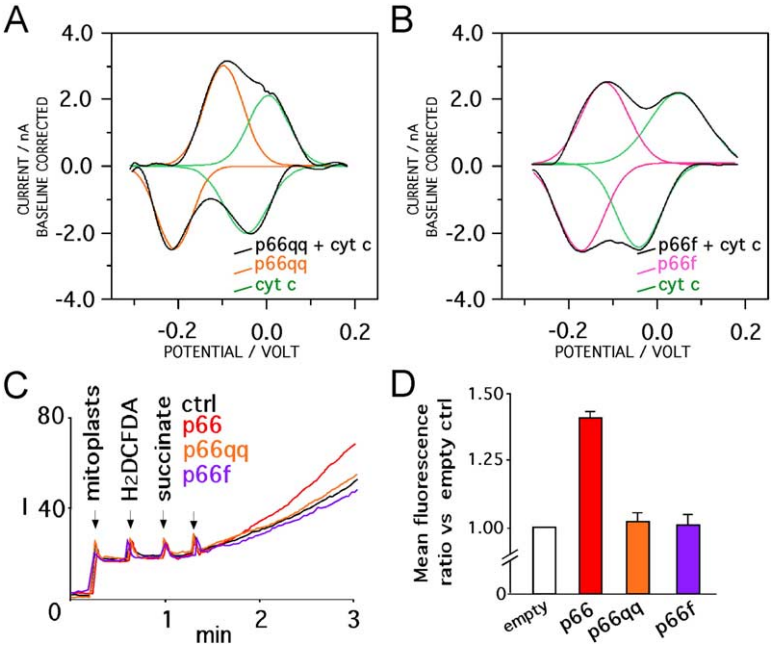

Figure 5. Impaired Redox Properties of p66Shc Mutants Defective for Cyt c Binding

(A) Voltammograms of cyt c (green), p66Shc*qq* (orange), and p66Shc*qq* + cyt c (black).

(B) Voltammograms of cyt c (green), p66Shc*f* (pink), and p66Shc*f* + cyt c (black).

(C) Fluorescence changes of purified liver mitoplasts during the sequential additions of H_2DCFDA; succinate; and buffer (ctrl, black), p66Shc (red), p66Shc*qq* (orange), or p66Shc*f* (violet) proteins.

(D) Ratio of the H_2DCFDA mean fluorescence, obtained by FACS analysis of p66Shc–/– MEFs after infection with control, p66Shc, p66Shc*qq*, or p66Shc*f* retroviruses; results are the average ± SEM of three experiments.

with cyt c (Zhen et al., 1999). We engineered similar mutations within p66Shc (p66ShcE132Q-E133Q mutation, p66Shc*qq*; p66ShcW134F mutation, p66Shc*f*) and evaluated their effects on the ability of the protein to bind cyt c, to transfer electrons, and to stimulate mitochondrial ROS generation. Notably, both *qq* and *f* mutations abrogated the ability of recombinant p66Shc to bind cyt c, as revealed by ELISA and pull-down experiments (Figures 4B and 4C).

The CV curves of the p66Shc*qq* and p66Shc*f* mutants showed symmetric peaks with redox potentials of –151 mV and –140 mV, respectively (Figures 5A and 5B). These values are markedly lower than that of wt p66Shc (–35 mV), suggesting that the E132-E133 and W134 residues influence the p66Shc redox properties. In the presence of cyt c, the CV responses of both mutant proteins resulted in two asymmetric peaks (Figures 5A and 5B), which could be easily deconvoluted into two components associated to the ET processes of cyt c (17 mV; Figures 5A and 5B, green traces) and the p66Shc*qq* (–150 mV; Figure 5A, orange trace) or p66Shc*f* (–141 mV; Figure 5B, pink trace) mutants. The detection of separated ET processes is consistent with a decreased interaction between the two p66Shc mutants and cyt c, as also revealed by ELISA and pull-down experiments (Figures 4B–4D). Therefore, both properties of executing ET and interacting with cyt c are impaired in the *qq* or *f* mutants of p66Shc, suggesting that the E132-E133 and W134 residues of p66Shc concur in the formation of its redox center and cyt c binding surface.

We then compared the ability of p66Shc, p66Shc*qq*, and p66Shc*f* to regulate production of ROS in vitro and in vivo. Addition of recombinant p66Shc*qq* and p66Shc*f* to digitonin-treated mitochondria did not increase H_2DCFDA oxidation (Figure 5C). Likewise, expression of p66Shc*qq* and and p66Shc*f* into p66Shc–/– MEFs did not increase the cellular fluorescence of H_2DCFDA-stained cells (Figure 5D). Therefore, mutations that impair the p66Shc redox center also inactivate the ability of p66Shc to stimulate ROS generation in vivo.

Mutation of the Redox Center of p66Shc Impairs its Ability to Mediate Mitochondrial Apoptosis

We then investigated whether the function of p66Shc to regulate mitochondrial apoptosis depends on its electrochemical properties, using the p66Shc*qq* mutant. To ensure that the *qq* mutation had not interfered with other functions of p66Shc, we first evaluated the ability of the two neighboring domains (PTB and CH2) to bind activated receptors and undergo phosphorylation after oxidative stress, respectively, and the property of p66Shc*qq* to localize within mitochondria. In the context of the *qq* mutation, the p66Shc PTB domain maintained its ability to bind activated EGF receptors (Figure 6A). Likewise, p66Shc*qq* was efficiently phosphorylated on serine following expression into p66Shc–/– MEFs and treatment with H_2O_2 (Figure 6B). Like the wt protein, p66Shc*qq* localizes within mitochondria (Figure 6C). Mitochondrial p66Shc is PK resistant (Figure 6D); it is released by digitonin treatment (Figure 6E) and forms a complex with mtHsp70, from which it dissociates after proapoptotic stimuli (Figure 6F).

We then measured the ability of the p66Shc*qq* mutant to regulate mitochondrial PT in vitro and apoptosis in vivo. P66Shc*qq* was unable to induce swelling of digitonized mitochondria (Figure 7A), nor did it restore the apoptotic response of p66Shc–/– MEFs upon treatment with H_2O_2 or staurosporine, as measured by cyt c release (Figure 7B), caspase activation (Figure 7C), and cell viability (Figure 7D). Notably, CsA inhibited the ability of reexpressed p66Shc to restore mitochondrial apoptosis following H_2O_2 (Figure 7E) or staurosporine (data not shown), supporting the theory that a functional PT is needed for the proapoptotic activity of p66Shc. It ap-

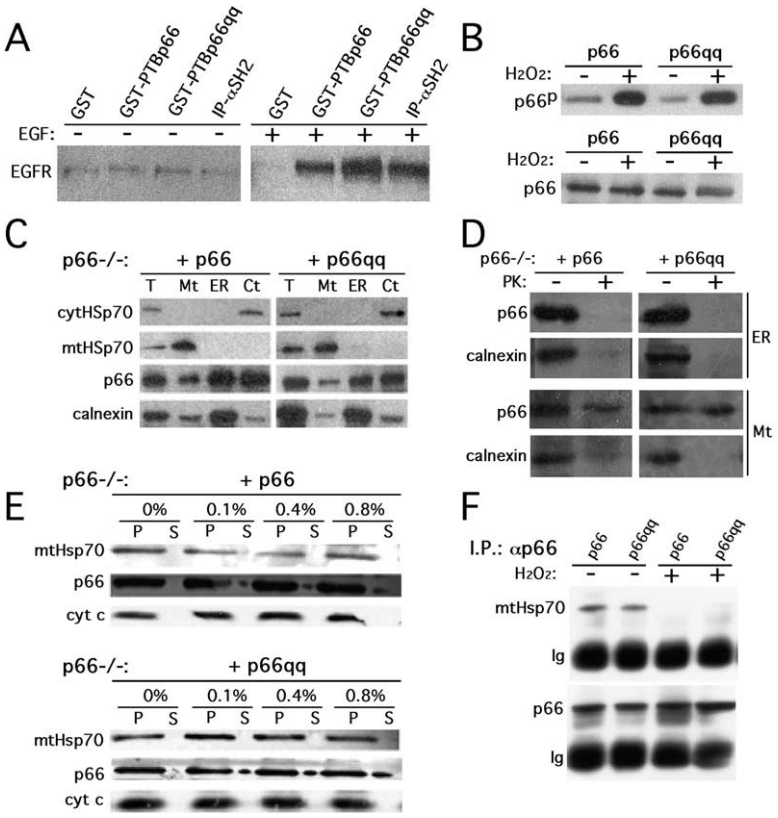

Figure 6. Receptor Binding, Phosphorylation, Localization, and Hsp70 Association of the p66^{Shc} Redox Mutants

(A) In vitro pull-down experiment using lysates of MEFs and treated or not with EGF, and GST, GST-PTBp66^{Shc}, or GST-PTBp66^{Shc}*qq*. Recovered proteins were analyzed by WB using anti-EGFR antibodies.

(B) P66$^{Shc-/-}$ MEFs were reconstituted with p66^{Shc} or p66^{Shc}*qq* by retroviral-mediated gene transfer and treated or not with H_2O_2. Anti-Shc immunoprecipitates were analyzed by WB using antibodies against phosphorylated p66^{Shc} (upper panel) or total pool of p66^{Shc} (lower panel).

(C) WB analysis of subcellular fractions from p66$^{Shc-/-}$ MEFs reexpressing p66^{Shc} or p66^{Shc}*qq*, using the indicated antibodies.

(D) Mitochondria (Mt) and ER-enriched fractions (ER) were treated with PK and analyzed by WB with indicated antibodies.

(E) MEFs mitochondrial fractions (as in [C]) were treated with the indicated concentrations of digitonin. After centrifugation, pellets (P) and supernatants (S) were analyzed by WB.

(F) MEFs mitochondrial fractions (as in [C]) were immunopreciptated with anti-p66^{Shc} antibodies. Specific immunoprecipitates were analyzed by WB using anti-mtHsp70 (upper panel) or anti-p66^{Shc} (lower panel) antibodies.

pears, therefore, that mutation of the p66^{Shc} redox center abrogates the functions of p66^{Shc} to induce mitochondrial PT in vitro and to mediate cellular apoptosis after stress.

Discussion

The present findings provide a mechanistic explanation for the proapoptotic function of p66^{Shc} and support a model whereby p66^{Shc} generates H_2O_2 within mitochondria, which, in turn, induces opening of the PTP and cellular apoptosis (Figure 8). ROS production by p66^{Shc} appears to be a specialized function whereby electrons are subtracted from the mitochondrial ETC to catalyze the partial reduction of molecular oxygen. This is the first demonstration that the mitochondrial respiratory chain can generate ROS not only accidentally but also through a specific enzymatic system. In this context, p66^{Shc} can be regarded as an atypical signal transducer that converts proapoptotic into redox signals.

In vitro and in vivo experiments demonstrated that p66^{Shc} oxidizes cyt c and generates H_2O_2. Therefore, a fraction of the mitochondrial electron flow, which is mostly used by COX to reduce oxygen to water, is deviated from cyt c by p66^{Shc} for the production of ROS (Figure 8). P66^{Shc} expression, however, does not influence the mitochondrial transmembrane potential under steady-state conditions, while it is indispensable for its collapse following proapoptotic signals (Orsini et al., 2004). These findings are compatible with the existence of two functional states of p66^{Shc}: inactive, under basal conditions, and active, after proapoptotic signals. A number of modifications of p66^{Shc} have been described, which occur within minutes after treatment with various proapoptotic signals and might lead to activation of p66^{Shc}: the cytosolic pool of p66^{Shc} becomes serine phosphorylated (Migliaccio et al., 1999), the mitochondrial pool of p66^{Shc} is released from a high molecular weight complex (Orsini et al., 2004), and both mitochondrial and cytosolic p66^{Shc} pools are increased (Trinei et al., 2002; Pacini et al., 2004). In the case of phosphorylation, genetic evidence indicates that this modification is required for the ability of p66^{Shc} to mediate apoptosis (Migliaccio et al., 1999). The underlying mechanism, however, is unknown. The mitochondrial pool of p66^{Shc} is not serine phosporylated (E.M. and F.O., unpublished data), and significant translocation of p66^{Shc} from cytosol to mitochondria does not occur after proapoptotic signals (Orsini et al., 2004), suggesting that serine phosphorylation might serve other, nonmitochondrial activities of p66^{Shc} that are also needed to exert its proapoptotic function. Mitochondrial p66^{Shc} exists within a high-molecular-weight complex, which includes members of the TIM-TOM import complex (TIM44, TIM20, TIM23, and mtHsp70; Orsini et al. [2004] and E.M. and F.O., unpublished data). The p66^{Shc}-mtHsp70 complex is destabilized following treatment with proapoptotic signals, leading to the release of monomeric p66^{Shc}. Since recombinant p66^{Shc} possesses constitutive redox activity, it is tempting to speculate that association with the TIM-TOM complex results with the inactivation of p66^{Shc} and that pro-

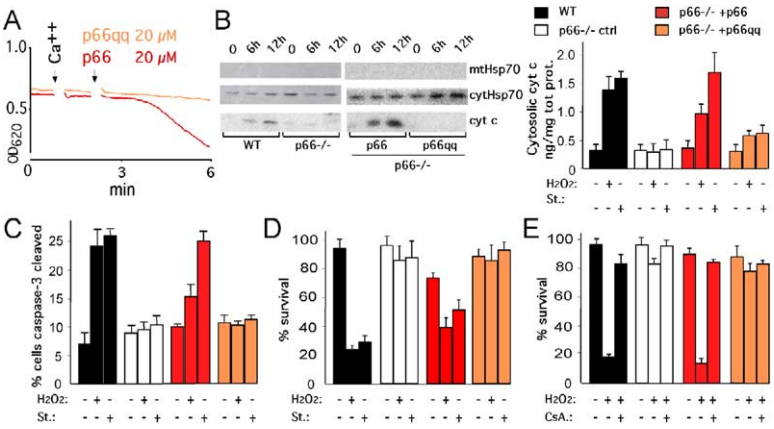

Figure 7. The p66Shc*qq* Mutant Does Not Induce PT, Nor Does It Activate Apoptosis

(A) Absorbance changes of digitonized liver mitochondria pretreated with Ca^{2+} and added of p66Shc (red trace) or p66Shc*qq* (orange) proteins.

(B) WT and p66Shc−/− MEFs infected with control, p66Shc, or p66Shc*qq* retroviruses were treated with 2 μM staurosporine and, after 6 or 12 hr, cytosolic fractions analyzed by WB (left panels). Cytosolic cyt c was analyzed by ELISA in the same cells after 6 hR treatment with 2 μM staurosporine or 800 μM H_2O_2 (right bar graph).

(C and D) The same cells as in (B) were treated with 2 μM staurosporine or 800 μM H_2O_2 and analyzed for caspase-3 activation (by flow cytometry using antibodies against cleaved caspase-3; [C]) or trypan blue (D).

(E) The same cells as in (B) were treated with H_2O_2 and 5 μm CsA and analyzed by trypan blue. Results represent the mean of triplicate cultures ± SEM.

apoptotic signals activate p66Shc by releasing it from this inhibitory complex.

A further mechanism of regulation of the proapoptotic function of mitochondrial p66Shc might be linked to its intrinsic redox properties. Since the calculated K_{eq} of the $[p66^{Shc}] + [cyt\ c] \leftrightarrow [p66^{Shc}]^- + [cyt\ c]^+$ redox reaction is 0.1, cyt c oxidation by p66Shc is unfavored when reduced cyt c is present at a concentration comparable to p66Shc. The reaction might, instead, occur if an excess of reduced cyt c is present, a condition that is achieved when COX activity is decreased (e.g., during hypoxia) or by physiological inhibition by nitric oxide (NO) (Sarti et al., 2003). Notably, reduced cyt c might also accumulate during tBid/Bax-induced apoptosis, since both molecules induce remodeling of the inner membrane and increase of free intermembrane cyt c (Scorrano et al., 2002), which is then fully reduced by the outer membrane rotenone-insensitive NADH-cyt b_5 reductase (Bernardi and Azzone, 1981). Therefore, different proapoptotic mechanisms may lead to increased concentrations of reduced cyt c, thus firing the ET reaction of p66Shc (Figure 8).

The levels of intracellular ROS and of oxidation-damaged DNA are significantly reduced in p66Shc−/− primary cultures (fibroblasts, endothelial cells, lymphocytes; Nemoto and Finkel [2002]; Trinei et al. [2002]; Zaccagnini et al. [2004]; Pacini et al. [2004]). Likewise, markers of oxidative stress (8-oxo-guanosine, isoprostane, nitrotyrosine) are decreased in tissues from p66Shc−/− mice (Trinei et al., 2002; Napoli et al., 2003; Francia et al., 2004), suggesting that p66Shc might regulate ROS production also in the absence of acute (proapoptotic) stress signals and that a fraction of intracellular ROS (and of oxidative stress) depends, under basal conditions, on the expression of p66Shc. Since p66Shc is activated by virtually every type of stress, the basal production of ROS by p66Shc may reflect its moderate activation by chronic stress. The redox balance has profound effects on metabolism and transcription, thus providing the molecular basis for a function of p66Shc

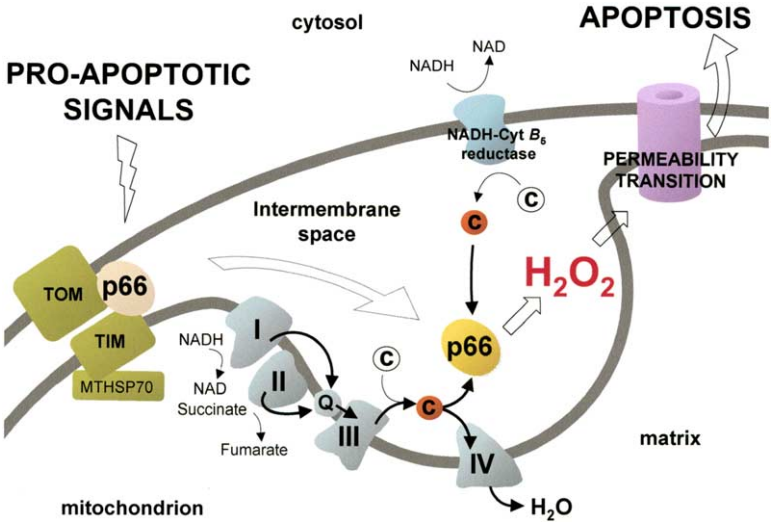

Figure 8. Model of p66Shc Redox Activity during Mitochondrial Apoptosis

Proapoptotic signals induce release of p66Shc from a putative inhibitory complex. Active p66Shc then oxidizes reduced cyt c (red) and catalyzes the reduction of O_2 to H_2O_2. PTP opening by H_2O_2 then leads to swelling and apoptosis. NADH-cyt b_5 reductase is indicated as additional putative source of reduced cyt c.

in the cellular adaptation to chronic stress. Regulation of redox equilibrium and apoptosis by $p66^{Shc}$ might equally contribute to its effect on life span.

Experimental Procedures

Cells, Vectors, and Antibodies

MEFs were treated with 2 μM staurosporine or 800 μM H_2O_2. Cytosolic cyt c was measured after 6 hr by ELISA and after 6/12 hr by WB of cytosolic fractions; anti-caspase-3 positive cells after 6 hr, by FACS; and cell survival after 20 hr, by trypan blue. Intracellular ROS were measured incubating cells for 30 min with 10 μM H_2DCFDA (Molecular Probes) in complete culture medium; cells were then recovered and suspended in PBS for FACS analysis. Mitoplast (0.5 mg/ml) or 0.4 mg/ml mitochondrial suspension and 30 μM DH_2CFDA were sequentially added to a spectrofluorimetric cuvette. Fluorescence (excitation wavelength [ex.] 498; emission wavelength [em.] 525) was registered using a Perkin Elmer Ls55 spectrofluorimeter at 25°C. Anti-$p66^{Shc}$ antibodies have been described (Orsini et al., 2004). Antibodies against caspase-3, mtHsp70, cytHsp70, calnexin, porin, phosphorylated $p66^{Shc}$ Ser36 residue, phosphotyrosine, and cyt c were obtained from commercial sources. The $p66^{Shc}$*qq* and *f* mutants were generated using the QuikChange Site-Directed Mutagenesis Kit (Stratagene) and cloned into the PINCO vector (Migliaccio et al., 1999).

Cellular Subfractionation, Mitochondria, and Mitoplast Preparation

Cell lysates were subjected to differential centrifugations to separate nuclei (700 rgf), mitochondria (8000 rgf), and the endoplasmic reticulum (15,000 rgf). Mice were intraperitoneally injected with 2 mg CCl_4/g of body weight CCl_4 20 hr before liver collection. Each mitochondrial preparation was assayed for respiration by using a Clark type oxygraph and swelling, as described (Petronilli et al., 1994), with minor modifications (OD_{620}; 0.4 mg/ml mitochondrial suspension with 5 mM succinate as substrate). Mitoplasts were obtained by hypotonic shock (1:10 dilution in deionized water for 5 min on ice).

Protein Film Voltammetry

We used a three electrode cell composed of a saturated calomel electrode (reference), platinum spiral wire (counter electrode), and gold disk (working electrode). The SAM was formed by soaking the gold electrode for 5 hr in 100 μM 11-mercaptoundecanoic acid. Purified horse cyt c (Sigma), $p66^{Shc}$, $p66^{Shc}$*qq*, or $p66^{Shc}$*f* solutions were deposited on the electrode surface and left to evaporate slowly. Measurements were performed in phosphate buffer and LiClO4 at constant ionic strength (100 mM). Before each experiment, the electrolyte solution was purged with argon transistor (lower than 1 ppm O2), and the voltammetric curves were recorded maintaining an argon blanket over the solution. CV experiments were carried out at 5–50 mV/s with an Autolab Model PGSTAT 30 at 25°C. Protein midpoint potentials (*E1/2*) were calculated as average between the potential of oxidation (*Epa*) and reduction (*Epc*) peaks.

Recombinant Proteins, ELISA, and In Vitro Binding Assay

All recombinant proteins were produced in *E. coli* as GST fusion proteins. GST was removed by prescission treatment after affinity column purification. For in vitro binding assays, total protein lysates (1 mg) were incubated for 2 hr at 4°C with 10 μg of the appropriate GST fusion protein. ELISA plates were coated with 4, 1, or 0.25 μg purified horse cyt c (Sigma) by using a 4 μg/ml coating solution in carbonate buffer (0.1 ml/well). After washing with PBS, different concentrations of recombinant Shc proteins were added to each well and incubated for 2 hr at 37°C. Binding was revealed using an anti SH2-SHC antibody (Transduction Laboratories) and horseradish peroxidase-conjugated anti-rabbit antibodies. Bound antibodies were detected using the TMB detection reagent (SIGMA).

Supplemental Data

Supplemental Data include four figures and can be found with this article online at http://www.cell.com/cgi/content/full/122/2/221/DC1.

Acknowledgments

We are grateful to S. Cattadori and D. Triarico for excellent technical support, C. Tacchetti and C. Puri for EM analysis, and V. Raker for some of the mitochondrial fractionation experiments. F.O. is recipient of a FIRC fellowship. This work was supported by grants from A.I.R.C. and M.I.U.R. M.G.; S.M., P.B., and P.G.P. are shareholders of Genextra Spa.

Received: November 10, 2004
Revised: March 22, 2005
Accepted: May 6, 2005
Published: July 28, 2005

References

Armstrong, F.A. (2002). Insights from protein film voltammetry into mechanisms of complex biological electron-transfer reactions. J. Chem. Soc., Dalton Trans. *5*, 661.

Balaban, R.S., Nemoto, S., and Finkel, T. (2005). Cell *120*, 483–495.

Becker, L.B. (2004). New concepts in reactive oxygen species and cardiovascular reperfusion physiology. Cardiovasc. Res. *61*, 461–470.

Bernardi, P., and Azzone, G.F. (1981). Cytochrome c as an electron shuttle between the outer and inner mitochondrial membranes. J. Biol. Chem. *256*, 7187–7192.

Bernardi, P., Petronilli, V., Di Lisa, F., and Forte, M. (2001). A mitochondrial perspective on cell death. Trends Biochem. Sci. *26*, 112–117.

Brownlee, M. (2001). Biochemistry and molecular cell biology of diabetic complications. Nature *414*, 813–820.

Cai, J., and Jones, D.P. (1998). Superoxide in apoptosis. Mitochondrial generation triggered by cytochrome c loss. J. Biol. Chem. *273*, 11401–11404.

Callegari, A., Cosnier, S., Marcaccio, M., Paolucci, D., Paolucci, M., Georgakilas, V., Tagmatarchis, N., Vázquez, E., and Prato, M. (2004). Functionalised single wall carbon nanotubes/polypyrrole composites for the preparation of amperometric glucose biosensors. J. Mat. Chem. *14*, 807–810.

Chance, B., Sies, H., and Boveris, A. (1979). Hydroperoxide metabolism in mammalian organs. Physiol. Rev. *59*, 527–605.

Chen, X., Ferrigno, R., Yang, J., and Whitesides, G.M. (2002). Redox properties of cytochrome c adsorbed on self-assembled monolayers: a probe for protein conformation and orientation. Langmuir *18*, 7009–7015.

Danial, N.N., and Korsmeyer, S.J. (2004). Cell death: critical control points. Cell *116*, 205–219.

Diwan, J.J., Yune, H.H., Bawa, R., Haley, T., and Mannella, C.A. (1988). Enhanced uptake of spermidine and methylglyoxal-bis(guanylhydrazone) by rat liver mitochondria following outer membrane lysis. Biochem. Pharmacol. *37*, 957–961.

Francia, P., delli Gatti, C., Bachschmid, M., Martin-Padura, I., Savoia, C., Migliaccio, E., Pelicci, P.G., Schiavoni, M., Luscher, T.F., Volpe, M., and Cosentino, F. (2004). Deletion of p66shc gene protects against age-related endothelial dysfunction. Circulation *110*, 2889–2895.

Green, D.R., and Kroemer, G. (2004). The pathophysiology of mitochondrial cell death. Science *305*, 626–629.

Griparic, L., van der Wel, N.N., Orozco, I.J., Peters, P.J., and van der Bliek, A.M. (2004). Loss of the intermembrane space protein Mgm1/OPA1 induces swelling and localized constrictions along the lengths of mitochondria. J. Biol. Chem. *279*, 18792–18798.

LeBel, C.P., Ischiropoulos, H., and Bondy, S.C. (1992). Evaluation of the probe 2′,7′-dichlorofluorescin as an indicator of reactive oxygen species formation and oxidative stress. Chem. Res. Toxicol. *5*, 227–231.

Mayer, M., and Noble, M. (1994). N-acetyl-L-cysteine is a pluripotent protector against cell death and enhancer of trophic factor-

mediated cell survival in vitro. Proc. Natl. Acad. Sci. USA *91*, 7496–7500.

Migliaccio, E., Mele, S., Salcini, A.E., Pelicci, G., Lai, K.M., Superti-Furga, G., Pawson, T., Di Fiore, P.P., Lanfrancone, L., and Pelicci, P.G. (1997). Opposite effects of the p52shc/p46shc and p66shc splicing isoforms on the EGF receptor-MAP kinase fos signalling pathway. EMBO J. *16*, 706–716.

Migliaccio, E., Giorgio, M., Mele, S., Pelicci, G., Reboldi, P., Pandolfi, P.P., Lanfrancone, L., and Pelicci, P.G. (1999). The p66shc adaptor protein controls oxidative stress response and life span in mammals. Nature *402*, 309–313.

Napoli, C., Martin-Padura, I., de Nigris, F., Giorgio, M., Mansueto, G., Somma, P., Condorelli, M., Sica, G., De Rosa, G., and Pelicci, P. (2003). Deletion of the p66Shc longevity gene reduces systemic and tissue oxidative stress, vascular cell apoptosis, and early atherogenesis in mice fed a high-fat diet. Proc. Natl. Acad. Sci. USA *18*, 2112–2116.

Nemoto, S., and Finkel, T. (2002). Redox regulation of forkhead proteins through a p66shc dependent signaling pathway. Science *295*, 2450–2452.

Orsini, F., Migliaccio, E., Moroni, M., Contursi, C., Raker, V.A., Piccini, D., Martin-Padura, I., Pelliccia, G., Trinei, M., Bono, M., et al. (2004). The lifespan determinant p66Shc localizes to mitochondria where it associates with mtHsp70 and regulates trans-membrane potential. J. Biol. Chem. *11*, 25689–25695.

Pacini, S., Pellegrini, M., Migliaccio, E., Patrussi, L., Ulivieri, C., Ventura, A., Carraro, F., Naldini, A., Lanfrancone, L., Pelicci, P., and Baldari, C.T. (2004). P66Shc promotes apoptosis and antagonizes mitogenic signaling in T cells. Mol. Cell. Biol. *24*, 1747–1757.

Pelicci, P.G. (2004). Do tumor-suppressive mechanisms contribute to organism aging by inducing stem cell senescence? J. Clin. Invest. *113*, 4–7.

Pelicci, G., Lanfrancone, L., Grignani, F., McGlade, J., Cavallo, F., Forni, G., Nicoletti, I., Grignani, F., Pawson, T., and Pelicci, P.G. (1992). A novel transforming protein (SHC) with an SH2 domain is implicated in mitogenic signal transduction. Cell *70*, 93–104.

Petronilli, V., Costantini, P., Scorrano, L., Colonna, R., Passamonti, S., and Bernardi, P. (1994). The voltage sensor of the mitochondrial permeability transition pore is tuned by the oxidation-reduction state of vicinal thiols. Increase of the gating potential by oxidants and its reversal by reducing agents. J. Biol. Chem. *269*, 16638–16642.

Sakon, S., Xue, X., Takekawa, M., Sasazuki, T., Okazaki, T., Kojima, Y., Piao, J.H., Yagita, H., Okumura, K., Doi, T., and Nakano, H. (2003). NF-kappaB inhibits TNF-induced accumulation of ROS that mediate prolonged MAPK activation and necrotic cell death. EMBO J. *22*, 3898–3909.

Sarti, P., Arese, M., Bacchi, A., Barone, M.C., Forte, E., Mastronicola, D., Brunori, M., and Giuffre, A. (2003). Nitric oxide and mitochondrial complex IV. IUBMB Life *55*, 605–611.

Scorrano, L., Ashiya, M., Buttle, K., Weiler, S., Oakes, S.A., Mannella, C.A., and Korsmeyer, S.J. (2002). A distinct pathway remodels mitochondrial cristae and mobilizes cytochrome c during apoptosis. Dev. Cell *2*, 55–67.

Scorrano, L., and Korsmeyer, S.J. (2003). Mechanisms of cytochrome c release by proapoptotic BCL-2 family members. Biochem. Biophys. Res. Commun. *304*, 437–444.

Trinei, M., Giorgio, M., Cicalese, A., Barozzi, S., Ventura, A., Migliaccio, E., Milia, E., Padura, I.M., Raker, V.A., Maccarana, M., et al. (2002). A p53-p66Shc signalling pathway controls intracellular redox status, levels of oxidation-damaged DNA and oxidative stress-induced apoptosis. Oncogene *21*, 3872–3878.

Ventura, A., Maccarana, M., Raker, V.A., and Pelicci, P.G. (2004). A cryptic targeting signal induces isoform-specific localization of p46Shc to mitochondria. J. Biol. Chem. *279*, 2299–2306.

Wallace, D.C. (1999). Mitochondrial diseases in man and mouse. Science *283*, 1482–1488.

Zaccagnini, G., Martelli, F., Fasanaro, P., Magenta, A., Gaetano, C., Di Carlo, A., Biglioli, P., Giorgio, M., Martin-Padura, I., Pelicci, P.G., and Capogrossi, M.C. (2004). P66ShcA modulates tissue response to hindlimb ischemia. Circulation *109*, 2917–2923.

Zhao, H., Kalivendi, S., Zhang, H., Joseph, J., Nithipatikom, K., Vasquez-Vivar, J., and Kalyanaraman, B. (2003). Superoxide reacts with hydroethidine but forms a fluorescent product that is distinctly different from ethidium: potential implications in intracellular fluorescence detection of superoxide. Free Radic. Biol. Med. *34*, 1359–1368.

Zhen, Y., Hoganson, C.W., Babcock, G.T., and Ferguson-Miller, S. (1999). Definition of the interaction domain for cytochrome *c* on cytochrome *c* oxidase. I. Biochemical, spectral, and kinetic characterization of surface mutants in subunit ii of Rhodobacter sphaeroides cytochrome aa(3). J. Biol. Chem. *274*, 38032–38041.